SICE Annual Conference 2012
August 20-23, 2012, Akita University, Akita, Japan

Remote Measurement Method of Surface Compliance Distribution for a Curved Surface Object

Masahiro Fujiwara and Hiroyuki Shinoda

Department of Information Physics and Computing, University of Tokyo, Tokyo, Japan
(Tel : +81-3-5841-6927; E-mail: {fujiwara,shino}@alab.t.u-tokyo.ac.jp)

Abstract: In this paper, we propose a method to measure surface compliance distribution of a curved surface object from a remote position for haptic information transmission. We achieve remote measurement by utilizing an ultrasound phased array. The measured surface compliance is estimated by information of distance and gradient dependencies of the acoustic radiation pressure. Finally, the measurement of a real object which has distributed surface compliance and reflectivity is performed.

Keywords: Compliance distribution, Remote measurement, Tactile sensing, Hardness evaluation, Haptic transmission.

1. INTRODUCTION

Remote measurement of surface compliance distribution is important for haptic transmission. A remote measurement system using acoustic radiation pressure for plane surface objects has been proposed in [1] as the first study. In this paper, we verify the effectiveness of the measurement system for curved surface objects. The surface compliance of a curved surface is estimated with a two step measurement. First, we measure the surface position and gradient optically. Then, we obtain the surface compliance from the surface displacement for a given acoustic radiation pressure considering the distance and gradient. The spatial distribution of the surface compliance is acquired by scanning the measuring point on the object surface. The effectiveness of proposed method is confirmed by applying measurement of surface compliance distribution of a fish head as a sample, which has distributed surface compliance, gradient, and optical reflectivity.

The contactless measurement of compliance or hardness has been approached in some researchers. To measure the compliance, it is necessary to apply force to the target mechanically and to obtain the response such as the displacement. A single method before [1] to measure the hardness of general objects in our daily life is to use air jet [2]. A problem of the method is it needs close location of the jet nozzle to the surface for a small radius jet nozzle. The proposed method in this paper enables remote measurement of surface compliance distribution including a curved surface object using ultrasound acoustic radiation pressure.

2. RELATED WORKS

Sensing methods of hardness or compliance are classified into two categories: direct and indirect measurement methods. The direct measurement method obtains hardness by pushing a target object actively and evaluating deformation of the object. This method calculates the hardness as the ratio of the pushing force to the deformation straightforwardly and the compliance is the reciprocal of the hardness. The indirect measurement method estimates the hardness of such a dynamic vibrated object from the observed resonant frequency or other specific parameters which includes hardness property. This indirect method has potential to acquire hardness property with a simple device, although a priori physical model and other properties such as mass or density distribution are required.

Furthermore, direct hardness measurement is classified from the viewpoint of the necessity for the contact between the sensor and the target object. Most hardness measurement systems have contact probes to push the object surface and measure the displacement. Elastography [3] using radiation pressure is included in contact methods. Meanwhile, demands for contactless measurement method exist widely for evaluation of fragile or delicate objects. In medical applications, hardness evaluation of tissue such as tumor gives critical information. Non-contact measurement of intraocular pressure does not give pain and is safer than contact method [4]. Besides, non-contact measurement of hardness is adequate to quality evaluation of raw foods such as meat, fish, vegetables, and fruits. Applying contactless method to this subject is not only sanitary, but also free from scratching them, and it also shortens measurement speed. Short time and non-constraining measurement of hardness provides the tactile information for a haptic transmission system. In this paper, we adopt a direct and non-contact remote measurement method of hardness or compliance distribution for mainly haptic transmission application. For haptic application, the measurement range of hardness should be around the skin hardness.

3. PRINCIPLE OF MEASUREMENT

3.1 Pressurization by acoustic radiation pressure

In this paper, surface compliance is defined as the ratio of vertical displacement to vertical force applied to a certain area in an object surface. Notice that the surface compliance depends on the pushed area. Since proposed system measures the displacement in haptic

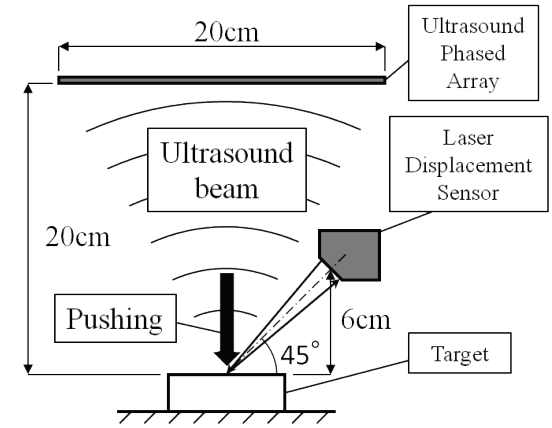

(a)

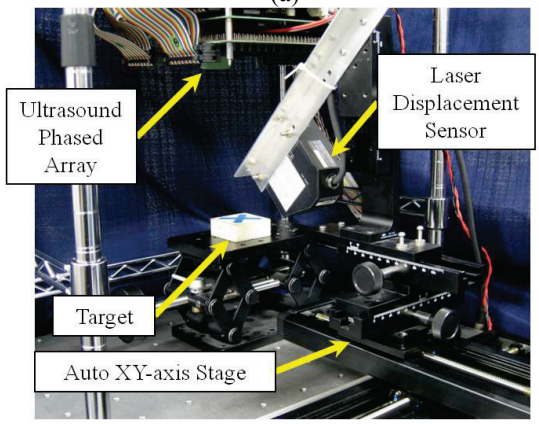

(b)

Fig.1: (a) Experimental setup of the proposed measurement system. (b) Appearance of the experimental setup.

interaction, we choose about 1cm diameter circle pushed area supposing a human finger pushes the surface.

We adopt acoustic radiation pressure, which is a non-linear phenomenon observed for large amplitude ultrasound, for non-contact pressurization of a target surface. In acoustics of linear range, the average of sound pressure becomes zero due to symmetry of expansion and compression rate of air. As amplitude becomes larger, asymmetry of those rates of air appears and the average of sound pressure has a positive bias. This biased pressure is called acoustic radiation pressure and allows us to push a surface of an object from a remote position. Unlike pressurization using air jet, it is easy to push a spot area of the target surface by using a converging beam with an ultrasound phased array.

The ultrasound phased array produces a specific wave-front of propagating ultrasound by controlling driving phases of each ultrasound transducer on the phased array. By generating the wave-front of convergent ultrasound beam, large amplitude ultrasound is produced at the focal point. Therefore, convergent ultrasound beam generated by the ultrasound phased array pushes the spot area on the target surface with the effect of acoustic radiation pressure by adjusting the focal point to that area. In that case, focal spot size can

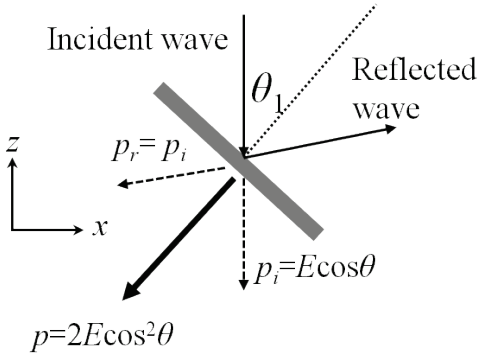

Fig.2: Ultrasound acoustic radiation pressure for oblique incidence to a perfectly reflective surface.

be comparable to the wave length of the propagating ultrasound at a sufficient aperture size that is comparable to or larger than the distance between the focal spot and the device.

The spatial distribution of the surface compliance of the target object is obtained at high-speed by using the ultrasound phased array because the pushed position on the area is changeable electronically. The updating time of the focal point depends on the processing frequency of the ultrasound phased array system. At the ultrasound phased array used in this research, the updating time is 0.25ms and it is limited by clock frequency of the FPGA in the system.

The proposed system consists of the ultrasound phased array and a laser displacement sensor based on triangulation as shown in Fig. 1. The distribution of the surface compliance is acquired by scanning the position of pushing and displacement sensing on the object surface. The scanning of the laser displacement sensor is achieved by an auto XY-axis mechanical stage and thus the updating rate of the measuring time is limited by the moving time of the stage.

3.2 Measurement for a curved surface

For the measurement of surface compliance distribution of a curved surface, the magnitude of acoustic radiation pressure on the target surface and measured displacement can be biased relying on positions on the surface. The bias is produced by distance variation between measurement system and the surface and by gradient variation of it. For removing the bias, the system needs information of the distance and gradient dependencies of acoustic radiation pressure and displacement sensing.

The gradient dependency of acoustic radiation pressure is obtained theoretically. The ultrasound acoustic radiation pressure $\vec{p}$ is determined as

$$\vec{p} = \vec{p}_i + \vec{p}_r \quad (1)$$

where $\vec{p}_i$ and $\vec{p}_r$ are incident and reflective components respectively. When an incident ultrasound to the surface at angle θ_1 is perfectly reflected as shown in Fig.2, the magnitude of the incident component of

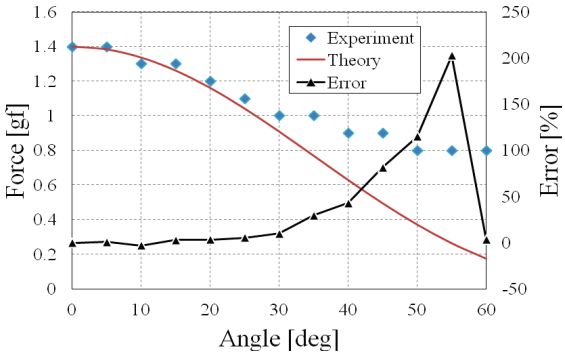

Fig.3: Experimental result of gradient dependency of force by ultrasound acoustic radiation pressure.

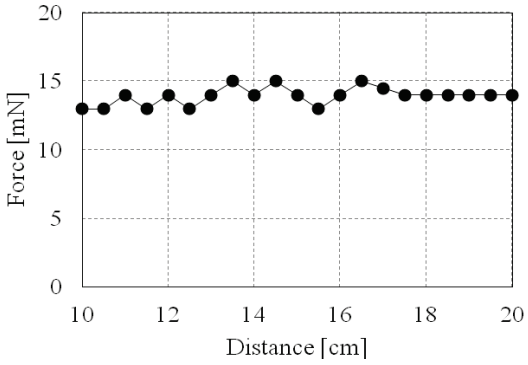

Fig.4: Experimental result of distance dependency of force by ultrasound acoustic radiation pressure.

acoustic radiation pressure is represented as

$$p_i = E\cos\theta_1 \quad (2)$$

where E is acoustic energy density near the surface. The direction of the spatial integrated acoustic radiation force is parallel to the propagation direction of incident ultrasound, regardless of the incident angle.

In perfectly reflective surface, the reflective acoustic energy is equal to the incident acoustic energy and thus the magnitude of the reflective component p_r is equal to the magnitude of the incident p_i. The direction of the reflective component is parallel to the propagation direction of reflected ultrasound. Therefore, the magnitude of total acoustic radiation pressure p is

$$p = 2E\cos^2\theta_1, \quad (3)$$

and its direction is normal to the surface. The radiation pressure is proportional to the square of $\cos\theta_1$ as shown by Eq.(3). Eq.(3) is utilized to calibrate the measured surface compliance data. The angle θ_1 is estimated by a height profile measured by the displacement sensor. The height profile of a line on the surface is given as $\{h_i\}_{i=1...N}$ measured at regular intervals by scanning of the displacement sensor. The maximum gradient angle θ_1 on a point i is approximated as $\theta_1=\mathrm{Tan}^{-1}\{(h_{i+1} - h_{i-1})/(2\delta)\}$, where δ is a scanning interval.

This quantification was confirmed by an experiment as shown in Fig.3. This result was obtained by pushing a tilted acrylic plate mounted on an electronic balance (EL1200, Shimadzu Corp.) using convergent ultrasound beam focused on the plate surface. In this case, expected force f along Z-direction measured by the electronic balance is

$$f = 2SE\cos^3\theta_1 \quad (4)$$

where S is the area of the focal point. Fig.3 shows the relative error of the experiment value from the theory is less than 10% up to 30deg. The relative error in the angle exceeding 30deg is not negligible.

It is derived by phased array theory that the distance dependency of the acoustic radiation pressure generated by an ultrasound phased array is almost constant along the vertical direction to the device surface. One concern is exponential absorptive attenuation of ultrasound in the air. The attenuation distance depends on the ultrasound frequency and the temperature of the air [5]. For example, at the 20 degree Celsius and 40kHz ultrasound, the attenuation rate is about 1dB/m. The attenuation rate increases as the ultrasound frequency rises. Therefore the frequency should be chosen taking account the required work distance from the device, which determines the size of the focal point.

A result of an experiment which confirms distance dependency is shown in Fig.4. Force due to ultrasound acoustic radiation pressure on the electronic balance is measured from 10cm to 20cm from the phased array. In this range, the force is 14mN±1mN and thus almost constant within 10% error.

The deviation of the measured displacement by a triangulation laser displacement sensor is corrected by the geometrical property of the sensor. The laser displacement sensor is attached to an auto XY-axis mechanical stage at the angle of 45 degrees to avoid the occlusion of ultrasound propagation as shown in Fig.1(a). In this case, measured (deviated) displacement y is represented from geometrical relationship as

$$y = -\frac{\sqrt{2}}{1+\tan\theta_2}x \quad (5)$$

where x is the true vertical displacement, and θ_2 is the angle between the laser direction of the sensor and the surface normal direction projected on the triangulation plane. Note that θ_2 relies on the arrangement of the displacement sensor against the target surface. The angle perpendicular to the triangulation plane does not affect the deviation of displacement sensing.

The relationship of Eq.(5) is confirmed by an experiment and the result is show in Fig.5. Fig.5(a) shows the experimental result as deviated displacement y against true displacement x changing surface angle from horizontal plane. The true displacement x was given by a manually driven Z-axis mechanical stage. In Fig.5(a), the deviated displacement y is proportional to the true displacement x as shown in Eq.(5). Fig.5(b) shows the experimental result and the theoretical curve of y against the surface angle θ_2 from horizontal plane, for various xs. These results indicate fine correspondence between actually measured values and theoretical ones given by Eq.(5).

It is performed that the total correction of the effect of the distance and gradient dependencies of the acoustic radiation pressure and the laser displacement sensor by Eq.(4) and Eq.(5). These experimental results of dependencies show that the correctable range of distance between the phased array and the target surface is from 10cm to 20 cm (covering all the range in the experiment) and that of angle is less than 30deg. The correctable angle range is confirmed by an experiment using a molded urethane gel sample as shown in Fig.6. The result of the experiment is shown in Fig.7. In the experiment, the distance between the phased array and the measured plane is 15cm. The normal surface compliance, whose surface angle is 0, is 1.14mm/N and it is expected that the value does not depend on the surface angle after correction. The measured surface compliance before correction is deviated for the angle more than 15deg. The corrected surface compliance maintains constant within 10% error up to the angle of 30deg. Therefore, the valid surface compliance value is given in these ranges by correcting the dependencies.

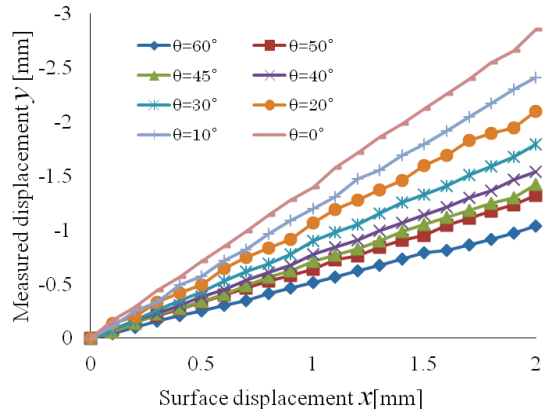

(a)

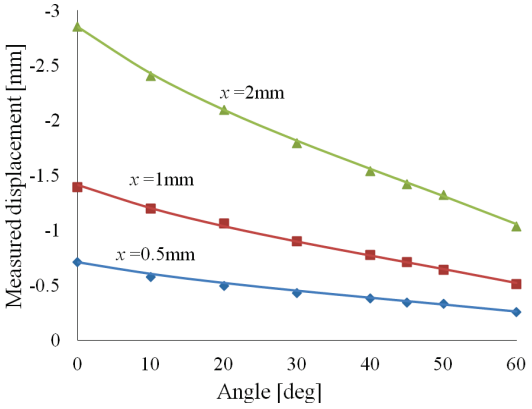

(b)

Fig.5: (a) Experimental relationship between measured displacement and true surface displacement. (b) Comparison of angle dependency between theoretical and experimental results.

4. EXPERIMENTS AND RESULTS

To verify the effectiveness of the measurement system, the surface compliance distribution of a curved real object is measured. The experimental set up is shown in Fig.1. The ultrasound phased array employed in this experiment is the identical to the one developed in [6]. Ultrasound transducers are arranged in a 18cm × 18cm substrate and transmit 40kHz ultrasound. Thus, the measurable distance range is about 36cm and the minimal size of the focal point is about 8.5mm, which is the wave length of the 40kHz ultrasound in the air of normal temperature. The size of the pushed spot area is almost equal to the focal size that is comparable to the human finger pad size. The target sample is 20cm distant from the ultrasound phased array so that the size of the focal becomes minimal.

The laser displacement sensor is scanned at 1mm interval by the auto XY-axis mechanical stage (SGSP26-200, SIGMA KOKI Corp). Since the repeat accuracy of the sensor is 0.2μm and the spatial integrated acoustic radiation pressure on the spot area is about 14mN, the resolution of the measured compliance is 14.3μm/N and the maximum measurement range of hardness is 70kN/m. It is necessary that the comparable surface compliance to human skin can be measured for haptic transmission. Because the hardness of the human

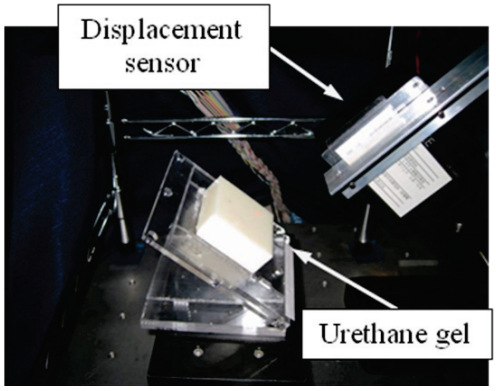

Fig.6: Appearance of experiment that confirms the validity of the correction for distance and gradient.

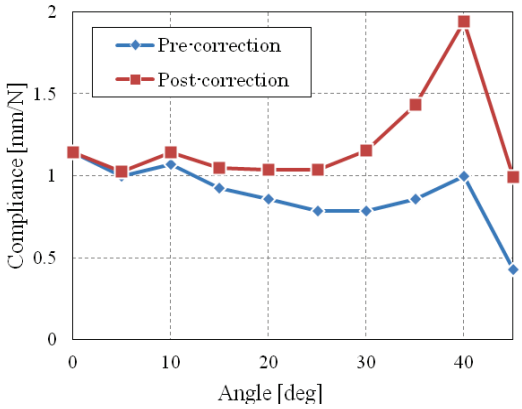

Fig.7: Correction result of surface compliance for the gradient of the object surface.

finger skin is less than 1.36kN/m [7], that measurement range is sufficient for haptic application.

The measured surface compliance distribution of a fish head (carangidae), which has a curved surface, is shown in Fig.8. The area of 4cm × 3cm is scanned at 1mm interval. The measurement time per a single point is 1s, so the total measurement time is about 20 minutes. That measurement time per a single point is determined by the time constant of the step response of the surface displacement for a step input of the radiation pressure.

The surface compliance distribution of a fish head is visualized in Fig.8. Characteristic surface compliance features are observed around the eye particularly. Although the reflectivity of the fish surface is ununiform and glittering, almost uniform distribution is obtained on the body (X<10mm). The estimated surface compliance and height profile along X-axis (Y=18.75mm) is shown in Fig.9. The surface compliance is high around X=21mm where the soft eye exists.

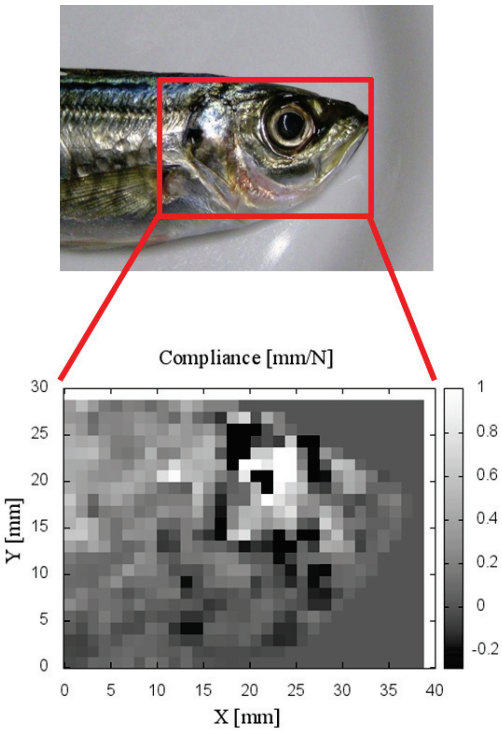

Fig.8: Measurement result of surface compliance distribution of a fish head (carangidae).

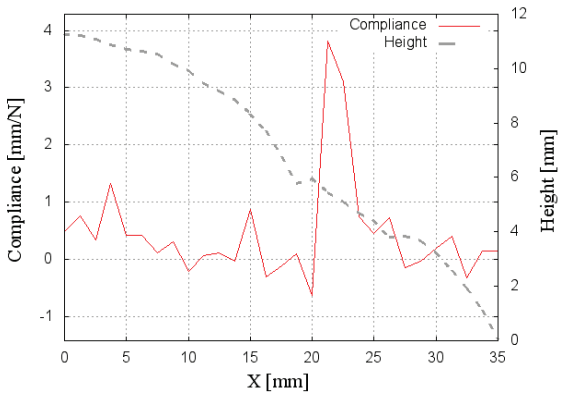

Fig.9: The surface compliance distribution and the height profile of the fish head against X-axis at Y = 18.75mm.

4. CONCLUSION

In this paper, we proposed a method to remotely evaluate the compliance distribution of a curved surface using ultrasound acoustic radiation pressure and verified the feasibility. The distance and gradient dependencies of the measurement system were quantified and confirmed by experiments. The valid surface compliance distribution is measured by correction with the dependencies. Finally, we measured a surface compliance distribution of a real object which has distributed surface compliance and reflectivity. As a future work, it is desirable to speed up the displacement measurement for utilizing the merit of the high speed pressurization by the ultrasound phased array.

REFERENCES

[1] M. Fujiwara, K. Nakatsuma, and H. Shinoda: "Remote Measurement of Surface Compliance Distribution for Haptic Broadcasting," *SICE Annual Conference 2011*, Tokyo, Japan, Sep. 2011.

[2] T. Kawahara, S. Tanaka, and M. Kaneko: "Non-Contact Stiffness Imager," *The International Journal of Robotics Research*, Vol. 25, No. 5-6, pp.537-549, May-June 2006.

[3] J. Ophir, I. Cespedes, H. Ponnekanti, Y. Yazdi, X. Li: "Elastography: A quantitative method for imaging the elasticity of biological tissues," *Ultrasonic Imaging*, Volume 13, Issue 2, pp. 111-134, April 1991.

[4] M. J. Moseley: "Non-contact tonometry," *Ophthalmic and Physiological Optics*, Vol. 15, Suppl. 2, pp. S35-S37, 1995.

[5] H. E. Bass, L. C. Sutherland, A. J. Zuckerwar, D. T. Blackstock, and D. M. Hester: "Atmospheric absorption of sound - Further developments," *Journal of the Acoustical Society of America*, Vol. 97, pp. 680-683, 1995.

[6] T. Hoshi, M. Takahashi, T. Iwamoto, and H. Shinoda: "Non-contact Tactile Display Based on Radiation Pressure of Airborne Ultrasound," *IEEE Transactions on Haptics*, Vol. 3, No. 3, pp.155-165, 2010.

[7] T. Maeno, K. Kobayashi and N. Yamazaki: "Relationship between the Structure of Human Finger Tissue and the Location of Tactile Receptors," *Bulletin of JSME International Journal*, Vol. 41, No. 1, C, pp. 94-100, 1998.